DEUTSCHES ELEKTRONEN-SYNCHROTRON DESY

DESY SR-72/13
July 1972

Inner Electron Excitation of Iodine in the Gaseous and Solid Phase

by

F. J. Comes, U. Nielsen, and W.H.E. Schwarz

2 HAMBURG 52 · NOTKESTIEG 1

To be sure that your preprints are promptly included in the HIGH ENERGY PHYSICS INDEX, send them to the following address (if possible by air mail):

DESY
Bibliothek
2 Hamburg 52
Notkestieg 1
Germany

Inner Electron Excitation of Iodine in the Gaseous and Solid Phase

F.J. Comes[+], U. Nielsen[++], and W.H.E. Schwarz[+++]

Deutsches Elektronen-Synchrotron DESY, Hamburg, Germany

The absorption spectra of gaseous and solid iodine have been measured in the photon energy range of 45 to 160 eV. The radiation of the 7.5 GeV electron synchrotron DESY was used as the light source. The intensity distribution of the 4d → εf continuum is discussed. A fine structure, similar in both phases, is found near the low-energy side of this continuum. This fine structure can be ascribed to transitions of $4d_{5/2}$ and $4d_{3/2}$ electrons into the lowest empty molecular orbital and into Rydberg states of the molecule. One-electron level energies and the $4d_{3/2}$, $4d_{5/2}$ ionization energies (58.95, 57.25 eV ± 0.2 eV) are deduced from the observed spectra. A rediscussion about the optical spectrum of the iodine molecule is given in the light of these results.

[+] Institut für Physikalische Chemie der Universität Bonn, Bonn, Germany

[++] II. Institut für Experimentalphysik der Universität Hamburg, Hamburg, Germany

[+++] Lehrstuhl für Theoretische Chemie der Universität Bonn, Bonn Germany

1. INTRODUCTION

Molecular iodine has been the subject of many investigations in the field of spectroscopy, its visible system being one of the most studied in molecular spectra. Many observations are concerned with experiments on the free particle in the gas phase.Due to its low-lying excited states much information on its electronic structure can be achieved, even in the visible and near infra-red. A good review of the work in the visible and near ultraviolet is given by Verma[1] and by Mathieson and Rees[2]. Mulliken[3] gave a detailed description of the different electronic configuration of the molecule and discussed the experimental data available until then. Recent observations by Venkateswarlu[4] cover the vacuum ultra-violet region between 1950 and 1250 Å with high resolution. Myer and Samson[5] extended the observations further down to 1050 Å, there joining the measurements of Yoshino et al.[6] who observed the absorption and photoionization from 1000 to 600 Å and 1000 to 750 Å, respectively.

During the last ten years interest in the electronic properties of molecular crystals has rapidly risen. Solid iodine forms molecular crystals which belong to the base-centered orthorombic system. These crystals, although molecular, show interesting semi-conducting properties. Photoconductivity measurements place the onset at 10 000 Å, which corresponds to a band gap of 1.24 eV[7]. Furthermore, as Brauner and Chen observed[8], absorption starts near 10 000 Å with a shift of the absorption edge to longer wavelengths with increasing temperature. Shimomura[9] measured the absorption spectrum of solid iodine from the near infra-red to the near ultraviolet and found a very broad and intensive absorption structure. Later experiments carried out by Schnepp, Rosenberg, and Gouterman[10] on single and oriented crystals with polarized light at low temperature (down to liquid helium) in the

region 7000 Å - 3000 Å showed four strongly polarized bands and one weakly polarized band. This same structure, although not so well resolved, was also found by Sobolev[11] in the reflection spectrum. The L_{III}-absorption spectrum of solid iodine at 2.7 Å was studied by Sigiura and Kiyono[12]. They refer to structures extending over a region of 16 eV from the absorption edge.

No measurements have been reported from the region of the extreme ultraviolet. In many cases they offer a more direct insight into the structure of the conduction band due to the narrowness of the initial bands and provide information on inner electron levels. Since the development of electron accelerators, such as the synchrotron, suitable light sources for the extreme ultraviolet have become available. The continuous emission spectrum extends from the visible far into the X-ray region so that one can now use this radiation in several laboratories to measure the optical properties of gaseous and solid compounds.

2. EXPERIMENTAL SET-UP

The radiation of the 7.5 GeV Deutsches Elektronen-Synchrotron DESY was used to investigate the absorption properties of gaseous and solid iodine. These properties were observed in the photon energy region 45 - 160 eV. An extension to lower and higher energies as far as 40 eV and 190 eV, respectively, was roughly carried out. The measurements were made with the aid of a one meter grazing incidence spectrometer providing a band width of 0.1 Å. The samples were installed into a special vacuum chamber placed before the entrance slit of the monochromator. In this chamber either a gas absorption cell or a cryostat with variable temperature could be mounted.

Details of the experimental set-up have been described in proceeding publications[13,15].

Solid iodine was prepared by evaporating iodine onto the surface of a thin film of carbon or aluminum mounted in the cryostat and cooled down to 80° K. The metal film served as both sample holder and ultraviolet radiation filter. Since a grating monochromator is used in combination with a light source of an extended emission spectrum, such as the synchrotron radiation, severe problems occur with spectra of higher orders. The use of carbon and aluminum filters in the wavelength region mentioned above reduce these problems to a high degree. Further reduction is achieved by the use of an additional concave mirror which deflects the primary beam by about 10° before entering the monochromator entrance slit.

The absorption cell has a length of 10 or 30 cm, respectively. It is provided with thin films of carbon or aluminum on both ends. Pumping of the cell is possible by a separate pumping system not connected to the main vacuum system. By these means no pressure drop along the light path in the cell occurs as is the case when using narrow slits and differential pumping.

A Bendix open photomultiplier provided with a tungsten photocathode (Model M 306) serves as the detector of the dispersed radiation. Its signal, biased to the signal of a second detector which is illuminated by part of the undispersed radiation, is amplified and fed into an xy-recorder whose x-axis is coupled to the wavelength drive of the spectrometer.

The normalization of the cross-sections to absolute values is based upon measurements with saturated iodine vapour at room temperature. Since the

thickness of the iodine layers in the low temperature experiments was not measured the cross section of solid iodine is given in relative units.

3. RESULTS AND DISCUSSION

Both the absorption of gaseous and solid iodine were measured. The curves are given in Figs. 1a and b. The succeeding figures are enlargements of those parts of the spectrum where fine structure occurs. The spectra for the gas and the solid are rather similar. This is especially true for the broad continuum with its maximum near 90 eV. But even the fine structure at lower energies shows some similarities. We will now discuss the results in more detail.

3.1 Continuous Absorption

The strong continuum with its maximum very near 93 eV is the most prominent feature in the extreme ultraviolet absorption spectrum of iodine in both phases. In the periodic table iodine and xenon are at neighbouring positions. As far as the continuous absorption is concerned similar absorption characteristics in the 100 eV region are expected for both elements. In the case of xenon a strong 4d → εf transition is observed, which is interpreted as a delayed onset due to the strong centrifugal barrier[13]. By inspecting our observations (Fig. 1) we can also interpret the strong continuous absorption in the region between 60 and 160 eV as being a 4d → εf transition. Although the shape of the observed continuum is determined by the molecular (or crystal) orbital in the initial and final states, the transition is mainly atomic in character and is only slightly affected by molecular formation

This is because the initial core MO's are nearly pure 4d orbitals which overlap with the continuum MO's mainly in the region of the atomic cores where these can be described by εf-atomic orbitals. Therefore, the contribution due to the cation and additional solid phase effects in the alkali crystals may be obtained by subtracting the absorption continuum of I_2, as given by Fig. 1, from the spectra of the alkali halides[14].

A second point in the discussion of the iodine continuous absorption is its absolute size and its integrated oscillator strength. From the spectrum (60 - 160 eV) one calculates an effective number of electrons between 5 and 6 for each iodine atom in the molecule. Similar numbers (6 - 7) are obtained from the spectra of the alkali halides[14] by tentatively adding up the contributions from the different ionic components. The behaviour of Cs^+ and Xe is contrary to this. Whereas the former contributes about 12 to 13 electrons to N_{eff}, xenon in the gas and solid phase[13] as well as in the fluorinated compounds XeF_2 and XeF_4[15] leads to $N_{eff} \approx 11$. Xe and Cs^+ exhibit a second low and broad maximum in the region between 200 and 700 eV also originating from 4d (and 4p) → εf transitions. Measurements in the soft X-ray region[16] together with calculations[17] conclude a contribution of 4d to N_{eff} of 3 and 1, respectively. In each case these numbers add up to about 14 for the total N_{eff} of 4d-transitions. This is the theoretically predicted number in the one-electron approximation[18].

When comparing N_{eff} of neighbouring elements it is interesting to look at the tellurium spectrum[29] from which a N_{eff}-value of about 10 is obtained for the first continuum hump. Its maximum height (23 Mb) is by 20 % lower than in xenon, whereas the second maximum near 300 eV is 25 % higher[16]. The measured N_{eff}-numbers for iodine do not fit in the general trend, but one

should remember that the possible errors in the measurements concerning the element as well as the alkali iodides are such that a 50 % higher value for N_{eff} might be possible.

For an explanation of the trend in going from Cs to Te the considerations by Cooper et al.[18,19] on the delayed onset of the continuous absorption should be remembered. The centrifugal forces contribute strongly to the effective potential as seen by the f AO's. Only electrons of sufficient kinetic energy are, therefore, able to cross this barrier. The 4d atomic orbital has its main maximum in the region of the potential minimum which is located at a smaller nuclear distance than the rotational barrier. If we go from Cs to Xe, I and Te the electrostatic potential decreases and the rotational barrier increases. The necessary kinetic energy at the absorption maximum thus grows from 25 eV (Cs) to 30 eV, (Xe), 35 eV (I), and nearly 40 eV (Te) as deduced from the spectra[13,14,29]. As a trend the 4d AO expands so that its main maximum moves further towards the rotational barrier (SCF-calculations of Mann[20]). As a result the overlap of the AO's of the 4d and the continuous of states with ε-values comparable to the barrier height becomes increasingly unfavourable. This causes the observed decrease in the maximum absorption of the first hump and an additional broadening. Obviously, the oscillator strength at higher energies has then to become larger.

Finally, we would like to comment on the fact (see Figs. 1a and 1b) that the solidification has hardly any influence on the continuous absorption in the region of the 4d → εf maximum. This same behaviour has already been observed with other molecules[14,21] as e.g. the xenon fluorides, SF_6 or others. The continuous absorption found in the spectra of the solid rare gases (Kr, Xe)[13] is different. Here a marked structure overlaps with the continuum. This is

very similar to the findings in the spectra of the alkali halides[14]. These structures can be described by metastable excitons (e.g. double electron excitations) and transitions to interband edges in the region of higher energies of the unoccupied bands.

The thus classified solids have two major different characteristics. In the one case the lattice elements are atoms or ions and in the other case molecules with internal vibrations. Whereas the lowest empty orbitals of the rare gases and alkali halides are Rydberg AO's, the molecules behave differently in so far as their lowest empty orbitals (LEMO's) are anti-bonding valence orbitals. The characteristic differences in the spectra mentioned above must, therefore, originate from the inherent differences in the lattice elements and not from the crystal forces. The higher excited states of the molecules in the solid are most likely mixed with the LEMO's. Through this the electronic excitation is strongly coupled to the molecular vibrations which result in a strong broadening effect. This is reflected by the spectrum of solid iodine in the energy region of 60 - 70 eV. The structure, as detected for gaseous iodine, is completely smeared out in the solid. The same effect has been observed for the xenon fluorides[15]. In contrast to this the solid rare gases and alkali halides show the well-resolved structure of the conduction band in this energy range.

3.2 Structured Absorption

The structures which occur in the iodine absorption spectrum can be arranged in three different groups (s. Fig. 1). They extend from 48 to 53 eV (region α), from 53 to 59 eV (region β), and from 59 eV up to higher energies into the continuum.

In region α (s. Fig. 2) two peaks of high intensity exist (A_1, A_2) having a half-width of 0.7 eV and an energy separation of ΔE = 1.68 eV. In the spectrum of the solid two peaks also occur, each accompanied by a smaller peak (B_1, B_2) on the high energy side (s. Fig. 3). In the case of B_1 it only appears as a shoulder of the A_2-peak.

In gaseous iodine, region β (Fig. 4) contains a series of lines C_1, D_1, E_1 and F_1, each with a width of only 0.25 eV and an additional series of 4 peaks at higher energies (ΔE = 1.7 eV) showing the same intensity relations as in the first series. It is evident that these two series of lines are caused by spin-orbit interaction in the 4d level. In the spectrum of the solid these peaks are smeared out to two broad humps with an energy separation of about 1.5 eV (s. Fig. 2). The strong broadening proves that the molecular transitions are of the Rydberg type.

In the region above 59 eV no structure was detected in the solid whereas three resonances occur in the gas (s. Figs. 1a and 2a). One very broad structure appeared at 60 to 63 eV, two somewhat narrower resonances at 74 eV and 82 eV. No structure could be observed at 125 eV and 185 eV where the 4p and 4s excitations should have occured.

The observed structures will be discussed on the following pages using the one-electron model which led to satisfactory results in the case of the xenon fluorides[15]. XeF_2 and I_2 are analogous molecules[+)]. We will, therefore, use the results from the xenon fluorides as leading terms in our discussion.

[+)] XeF_2 may be looked upon as a halogene molecule with a large interatomic distance containing a heavy nucleus.

3.2.1 Region α

By molecular formation the initial 4d AO's of the iodine atoms split into σ_g, σ_u, π_u, π_g, δ_g, δ_u molecular orbitals. The core AO's hardly overlap. Contrary to the XeF_2 case the charge distribution will change only a little on formation of the molecule so that the resulting "ligand field splitting" is certainly below 0.1 eV; it will, therefore, not be considered in the discussion on the spectra. Obviously, the observed separation of 1.68 eV between the two peaks A_1 and A_2 is to be interpreted as 4d spin-orbit splitting of iodine. It is very near the calculated and estimated values ranging from 1.7 to 1.8 eV[14,22,23] and those observed from the alkali halides (1.5 to 1.8 eV)[14,33]. ESCA measurements on KI yield a splitting of 1.6 eV[23]. The interpretation of A_1 and A_2 as spin orbit mates is further well supported by the measured intensity ratio of 1.4 ± 0.1 for the two peaks; for a transition from the $4d_{3/2,\ 5/2}$ levels into the lowest empty MO (LEMO) we expect an intensity ratio of 1.5 for the two absorption lines. The small difference to the measured intensity ratio shows that the two-electron interaction is indeed rather small and justifies the use of the one-electron model.

The lowest empty MO is an anti-bonding (I-$5p_o$) σ_u valence orbital. We expect that due to this the absorption will be vibrationally broadened and shifted to higher energies by 0.5 to 1 eV; this is estimated from the observed line width of the A_1, A_2 peaks. In order to calculate the shift ΔE_{vib} we used a vibrational frequency of 200 cm^{-1} in both states and a stretching of the bond upon excitation of 0.4 Å. These values are reasonable according to spectroscopic data on I_2[24] and lead to ΔE_{vib} = 0.75 eV. The measured difference in the adiabatic and vertical energy of the electron affinity of I_2[25] (0.7 eV) supports the discussed shift of the lines.

In order to get the orbital energies of $4d_{3/2,5/2}$ we need the energy of the LEMO. The latter can be deduced from the optical spectrum in the ultraviolet. The $(\pi_g^3\ \pi_u)^3\Pi_{u1}$ state has an excitation energy of 1.5 eV. The ionization potential of I_2 is at 9.4 eV ($\pi_g^3\ ^2\Pi_{g1/2}$), and at 10.0 eV ($\pi_g^3\ ^2\Pi_{g3/2}$), respectively. This leads to a binding energy of 8 to 8.5 eV for the σ_u orbital from which an ionization energy of 57 and 58.5 ± 1 eV is deduced for the 4d electrons. These values are near the corrected+) SCF-values[20] of 58.4 and 60.1 eV and those taken from the β-region (57.25 eV and 58.95 eV) as explained in detail below.

4d binding energies as given in the references differ by more than 5 eV. ESCA measurements[23] lead to a mean value of 54 eV for the 4d ionization energy of neutral iodine. But the ESCA results obtained by different authors[23,27] for the 3d binding energy are not consistent. New ESCA measurements of iodine are, therefore, recommended.

Let us now look at the spectrum of solid iodine in the same energy region (Fig. 3). Here we have 4 peaks ($A_{1,2}$, $B_{1,2}$) where the two A_1 and A_2 are of equal size and at the same position as in the gaseous sample. This is expected for a transition into the valence shell (Frenckel exciton). The smaller peaks at the high energy side of $A_{1,2}$ might be Wannier excitons of n = 2. Their intensity is about 1/8 of that of the main peaks. Energetic reasons could also explain the absorption by using a $(4d^9)\ I_2^+ - (5p_o\ \sigma_u)\ I_2^-$ ion pair (charge-transfer exciton). Both interpretations are of similar physical merit: a σ_u (n = 2) Wannier exciton has its density maximum at a distance of 6 Å in the axis of the I_2 molecule (assumed value of the dielectric constant of I_2 : 3). In this direction the distance between the molecular centers of nearest neighbours in the iodine crystal is 5 Å[28].

+) The correction factor is the same as the one which fits the experimental[26] and SCF-results[20] in the case of xenon.

3.2.2 Region β in Gaseous Iodine

Unfortunately no MO-calculations exist for I_2. But qualitative predictions on the empty MO's can be made with the aid of the correlation diagram given in Fig. 5 and the known order of Rydberg orbitals in the lighter diatomics[30].

The orbital energies of the n = 6 shell of the iodine atom are 3.1 (s), 2.0 (p) and 1.6 (d) eV[31]. Spin-orbit splitting of the Rydberg levels is negligible. The lowest Rydberg orbital in the molecule will be of the σ_g - 6s type, originating preferentially from the 6s AO's. We estimate the orbital energy ε to lie between -3 and -3.5 eV. The Rydberg orbitals which follow in energy scale are the $b\sigma_u$, $a\pi_u$, $a\pi_g$-MO's correlating with the 6s and 6p AO's. They are of 6p and 5d Rydberg character. Their binding energy is expected to be nearly 2 eV. As far as the order of these orbitals is concerned strict predictions cannot be made on the basis of a qualitative inspection. Higher orbitals in the region of -1.5 eV are the $c\sigma_u$-MO correlating with the $6p_o$-AO's, which behave as a 4f Rydberg MO, and other ones, which correlate with the 5d-AO's.

A remark should be made concerning the 5d- and 4d Rydberg MO's. If we look at the diagram (Fig. 5) we see that some of the molecular d and f levels have much lower energy than the corresponding Rydberg levels in the free atom. Only at large distances from the molecular center do those molecular orbitals behave as d and f orbitals. In the region of the atomic cores, however, they can be approximated by s, p (and d) AO's. According to this the corresponding 4d - nd and 4d - nf Rydberg transitions will have a noticeable intensity in the case of the molecule whereas they are Laporte-forbidden or extremely weak in the atom.

From the foregoing energy-considerations we will tentatively make the assignments given in Table I. They are supported by the intensities of the absorption peaks. The intensity ratio of the two groups of lines is approximately 3:2 as is expected for spin-orbit mates. Within one group the intensities follow along the line of being higher with an incraesing number of possible transitions. But the C-peaks ($4d \rightarrow a\sigma_g$-transition) are still further weakened. As mentioned above, the main component of the $a\sigma_g$-MO in the region of the atomic core is a 6s AO which has a vanishing transition moment with the initial 4d core orbitals.

If the scheme as given in Table I is correct we can calculate relative orbital energies from the observed spectrum. Absolute values are then obtained from comparison with the estimated values as given above and from the interpretation of the D- and F-peaks as being members of a Rydberg series. They are given in Table II. The estimated accuracy is ± 0.2 eV.

3.2.3 Excitations above 59 eV in Gaseous Iodine

As the experimental results connected with these transitions are rather uncharacteristic the interpretation is more or less speculative. We observe two broad "lines" (γ,δ) at 11 and 24 eV above the $4d \rightarrow$ LEMO-excitation. Energetically γ and also δ could arise from an additional excitation of the valence shell. Transitions from the $5p\sigma_g$, π_u, π_g-valence MO's into the LEMO should exhibit energies of about 10 eV (γ). For such two-electron transitions no narrow absorption lines are expected. The δ peaks may be ascribed to an additional excitation of a $5s\sigma$-electron which presumably needs 20 - 25 eV. The η peak at 8 eV above the δ-peak could arise from a (4d, 5s)-tow-electron excitation with both electrons excited to Rydberg orbitals. Table III summarizes these interpretations.

Findings in the spectra of the rare gases krypton and xenon are similar[13]. There structures exist which overlap with the continuous 3d and 4d excitations. Codling and Madden[32] have assigned these structures as being double electron excitations. In the spectra of the alkali halides similar structures in the strong continuum are observed. Generally, double excitations have only small transition probabilities, much lower than would be observable in these absorption spectra. But the examples discussed above are exceptional since the continuous absorption is very strong. Only little configuration mixing of the single excited continuous and the double excited discrete states is sufficient to cause an oscillator strength comparable to that of the Rydberg single excitations.

3.3 Comparison with Results from Valence Shell Excitations

A large number of absorption lines of the iodine spectrum has been assigned by Venkateswarlu[4]. Besides other transitions five Rydberg series converging at the ionic ground states $^2\Pi_{g\ 3/2,1/2}$ have been observed. We shall prove the usefulness of the one-electron model applied in the foregoing chapters for the interpretation of the XUV-spectrum to describe also these valence shell excitations. The one-electron energies thus obtained will support the assignment given in Table I. One the other hand it will, furthermore, be possible to comment on the more tentative interpretation Venkateswarlu has given to several valence excitations.

The electronic ground state of I_2 is $(\ldots \pi_u^4 \pi_g^4)\ ^1\Sigma_g^+$. Rydberg levels converging to the $(\ldots \pi_u^4 \pi_g^3)\ ^2\Pi_{g\ 3/2,1/2}$ ionization limits are given in Table IV as assigned by Venkateswarlu. We find that the measured Rydberg energies can be calculated within 0.1 eV with the aid of the one-electron

model. Since the interaction of the Rydberg electron with the open valence shell is certainly stronger than with the 4d-hole this gives further confidence for the correctness of the description of the XUV-spectrum by means of the one-electron model. Furthermore, we see that the one-electron energies obtained from the XUV-spectrum are different from the values given in Table IV by not more than 0.1 eV, only the 7p-energy value deviating by 0.15 - 0.20 eV.

Besides the Rydberg states already discussed Venkateswarlu has tentatively assingned another 22 states which are presumably also Rydberg states. They are members of series converging at higher ionization limits as $(\ldots \pi_u^3 \pi_g^4)$ $^2\Pi_{u\ 3/2,1/2}$ and $(\ldots \pi_u^4 \pi_g^2 \sigma_u)$ $^4\Sigma_u^-$, $^2\Delta_u$, $^2\Sigma_u^+$. The consequences of Venkateswarlu's assignments are given in Table V. From this we come to the following conclusion about the interpretation of the spectrum: the assignment of the σ_g6s-Rydberg levels seems to be correct. The deduced IPs for the $(\ldots \pi_u^4 \pi_g^2 \sigma_u)$-configuration are reasonable. The other assignments are rather doubtful. This is especially true for the progressions named m, p, v, w and probably n, which is explained in the footnotes of Table V.

4. CONCLUDING REMARKS

The proceeding discussion has given at least a qualitative interpretation of the spectrum of gaseous and solid iodine in the energy region between 40 and 190 eV. Values of the 4d-ionization potentials could be extracted from the spectra. They are very different from those given by ESCA-measurements. The spin-orbit splitting of the 4d subshell is deduced from the observations. The discussion of the molecular Rydberg states point out the necessity of reinterpreting the optical spectra. Through lack of detailed

structure in the range of continuous absorption of solid iodine no essential remarks on the structure of the conduction band could be deduced from the observations in the XUV. An interesting relation between the oscillator strength of the 4d-ionization continuum and the nuclear charge as observed from the meaurements is discussed. This point needs further experimental and theoretical work. The problem of double electron excitation in the presence of strong continua is another point which needs more theoretical research. The experimental results should also be refined.

ACKNOWLEDGMENT

It is a pleasure to thank Prof. R. Haensel for many discussions. One of the authors (F.J.C.) is grateful to the DESY Board of Directors for making a five months stay in Hamburg possible.

Figure Captions

Fig. 1 Cross-section of gaseous (a) and solid (b) I_2 versus photon energy in the energy range of 45 - 160 eV.

Fig. 2 Cross-section of gaseous (a) and solid (b) Iodine versus photon energy in the energy range of 45 - 72 eV.

Fig. 3 Cross-section of solid Iodine in the energy region of 48.5 - 53 eV.

Fig. 4 Cross-section of gaseous Iodine in the energy region of 53 - 59 eV.

Fig. 5 Rydberg orbital diagram of Iodine (schematic)

References

1. R.D. Verma, Proc. Indian Acad. Sci., Sect. A., 48, 197 (1958); J.Chem.Phys. 32, 738 (1960)
2. L. Mathieson and A.L.G. Rees, J.Chem.Phys. 25, 753 (1956)
3. R.S. Mulliken, Phys.Rev. 46, 549 (1934); 57, 500 (1940)
4. P. Venkateswarlu, Can.J.Phys. 48, 1055 (1970)
5. J. Myer and J.A.R. Samson, J.Chem.Phys. 52, 716 (1970)
6. M. Yoshino, A. Ida, K. Wakiya and H. Suzuki, J.Phys.Soc.Japan 27, 976 (1969)
7. T.S. Moss, Photoconductivity of the Elements, (Butterworth Scientific Publications Ltd., London 1952)
8. A.A. Brauner and R. Chen, J.Phys.Chem. Solids 24, 135 (1963)
9. K. Shimomura, J.Phys.Soc.Japan 14, 235 (1959)
10. O. Schnepp, J.L. Rosenberg and M. Gouterman, J.Chem.Phys. 43, 2767 (1965)
11. V.V. Sobolev, Sov.Phys.-Semicond. 4, 843 (1970)
12. C. Sigiura and S. Kiyono, Techn.Rep., Tohoku Univ. 32, 75 (1967)
13. R. Haensel, G. Keitel, P.Schreiber and C. Kunz, Phys.Rev. 188, 1375 (1969)
14. M. Cardona, R. Haensel, D.W. Lynch and B. Sonntag, Phys.Rev. B2, 1117 (1970)
    F.C. Brown, C. Gähwiller, H. Fujita, A.B. Kunz, W. Scheitley and N. Carrera, Phys.Rev. B2, 2126 (1970)
15. F.J. Comes, R. Haensel, U. Nielsen and W.H.E. Schwarz, to be published

16. A.P. Lukirskii, I.A. Brytov and T.M. Zimkina, Opt.Spektrosk. 17, 438 (1964), engl. transl. p. 234
A.P. Lukirskii, I.A. Brytov and S.A. Gribovskij, Opt.Spektrosk. 20, 368 (1966), engl. transl. p. 203
17. D.J. Kennedy, S.T. Manson, Phys.Rev. A5, 227 (1972)
18. U. Fano and J.W. Cooper, Rev.Mod.Phys. 40, 441 (1968)
19. J.W. Cooper, Phys.Rev.Letters 13, 762 (1964)
20. J.B. Mann, Atomic Structure Calculations, Los Alamos, University of California 1968
21. D.Blechschmidt, E.E. Koch, R. Haensel, U. Nielsen and T. Sagawa, Chem.Phys.Letters,14,33(1972)
22. A.B. Kunz, J.Phys.Chem.Solids 31, 265 (1970)
23. K. Siegbahn, C. Nordling, A. Fahlman, R. Nordberg, K.Hamrin, J. Hedman, G. Johansson, T. Bergmark, S.-E. Karlsson, I. Lindgren, B. Lindberg, ESCA, Uppsala 1967
24. G. Herzberg, Molecular Spectra and Molecular Structure I, Princeton, Van Nostrand 1950
25. W.B. Person, J.Chem.Phys. 36, 109 (1963)
26. K. Codling and R.P. Madden, Phys.Rev. Letters 12, 106 (1964)
27. W. Brügel, private communication
28. A.I. Kitaigorodskij, T.I. Chotsyjanova and Y.T. Strutschkov, J.Fis.Chim. (russ.) 27, 780 (1953)
29. T. Tuomi, B. Sonntag, G. Zimmerer and K. Maschke, to be published
30. T. Betts and V. McKoy, J.Chem.Phys. 54, 113 (1971)
31. C.E. Moore, Atomic Energy Levels, III. NBS Circular 467, 1958
32. K. Codling and R.P. Madden, Appl.Opt. 4, 1431 (1965)
33. T.M. Zimkina, V.A. Fomichev, Fis.Tvjerd.Tjela 10, 1392 (1968)
34. D.C. Frost, C.A. McDowell and D.A. Vroom, J.Chem.Phys. 46, 4255 (1967)

Tab. I Peaks in the Spectrum of Iodine

gas			solid		
peak	energy (eV)	assignement	peak	energy (eV)	assignement
A_1	49.27	$4d_{5/2} \rightarrow (5p)\sigma_u$	A_1	49.27	$4d_{5/2} \rightarrow (5p)\sigma_u$ Frenkel-exciton
			B_1	~50.5	n = 2 Wannier exciton or charge transfer exciton
A_2	50.93	$4d_{3/2} \rightarrow (5p)\sigma_u$	A_2	50.93	$4d_{3/2} \rightarrow (5p)\sigma_u$ Frenkel-exciton
			B_2	52.16	n = 2 Wannier exciton or charge transfer exciton
C_1	54.05	$4d_{5/2} \rightarrow \sigma_g 6s$			
D_1	55.08	$4d_{5/2} \rightarrow \sigma_u, \pi_u 6p$ and $\sigma_g, \pi_g 5d$	B_1	55.3	$4d_{5/2} \rightarrow$ conduction band
E_1	55.70	$4d_{5/2} \rightarrow \sigma_u, \pi_u 4f$			
F_1	56.29	$4d_{5/2} \rightarrow 7p, \ldots$			
C_2	55.80	$4d_{3/2} \rightarrow \sigma_g 6s$			
D_2	56.76	$4d_{3/2} \rightarrow \sigma_u, \pi_u 6p$ and $g, \pi_g 5d$	B_2	56.8	$4d_{3/2} \rightarrow$ conduction band
E_2	57.40	$4d_{3/2} \rightarrow \sigma_u, \pi_u 4f$			
F_2	58.01	$4d_{3/2} \rightarrow 7p, \ldots$			

Tab. II One-electron energy levels of I_2

level	energy in eV (absolute values)
$^4d_{3/2}$	58.95
$^4d_{5/2}$	57.25
$5p\sigma_u$	8.5 - 9.0 (vertical: 8.0)
$\sigma_g 6s$	3.15
$\sigma_u, \pi_u 6p$	2.2
$\sigma_g, \pi_g 5d$	
$\sigma_u, \pi_u 4f$	1.5_5
7p	0.9_5
ionization limit	±0.2

Tab. III Structures in the Iodine-Spectrum

structure	mean energy (eV)	interpretation
α	50	4d ⟶ LEMO
β	56	4d ⟶ Rydberg orbital (conduction band)
γ	~ 61	(4d,5p) ⟶ (LEMO)
δ	74	(4d,5s) ⟶ (LEMO)
η	82	(4d,5s) ⟶ (Rydberg orbitals)

Tab. IV One-electron energy levels from valence electron excitations

Orbital of the excited electron	symbol and energy of the excited I_2-state according to Venkateswarlu [4]		corresponding one-electron energies* (absolute value in eV) and higher Rydberg levels (principal quantum number in parenthesis)		
	$^2\Pi_{g\ 3/2}$-core	$^2\Pi_{g\ 1/2}$-core			
$5p_o\ \sigma_u$	A 1.46	B 1.95	8.0		
$\sigma_g 6s$	a 6.39	b 6.94	3.05 ± .04		
$q_u 6p_o$	c 7.06	f 7.77	2.30 ± .04	1.15 ± .02 (7)	0.69 (8)
$\pi_u 6p_{\pm1}$	d 7.17 e 7.31	i 7.88 j 7.97	2.13 ± .1	1.09 ± .01 (7)	0.66 (8)
$\sigma_u 4f_o$	g 7.84	o 8.37 o'8.40	1.61 ± .05	0.89 ± .02 (5)	0.55 (6)
$\pi_u 4f_{\pm1}$	k 7.98	q 8.42 r 8.61	1.48 ± .1	0.83 ± .05 (5)	0.53 (6)
$\delta_u 4f_{\pm2}$	l 8.03	s'8.69 s 8.73	1.34 ± .03	0.78 ± .02 (5)	0.51 (6)

* calculated from Venkateswarlu's I.P. of 9.40 eV ($^2\Pi_{g\ 3/2}$) and 10.03 ($^2\Pi_{g\ 1/2}$)

Tab. V Rydberg States according to Venkateswarlu [4]

Rydberg orbital	core state	symbol and energy (eV)	conclusion
$\sigma_g 6s$	$^2\Pi_{u\ 3/2}$	h 7.88	$\varepsilon(\sigma_g 6s) = 3.06$ eV[a,d]
	$^2\Pi_{u\ 1/2}$	t,t' 8.80	$\varepsilon(\sigma_g 6s) = 2.95$ eV[a,d]
	$^4\Sigma_u^-$	α 7.68	IP ($^4\Sigma_u^-$) = 10.75 eV[b,d]
	$^2\Sigma_u^+$	γ 8.48 δ 8.58	IP ($^2\Sigma_u^+$) = 11.6 eV[b,d]
	$^2\Sigma_u^-$	δ,δ' 8.64	IP ($^2\Sigma_u^-$) = 11.7 eV[b,d]
$\sigma_g 5d_o$	$^2\Pi_{u\ 3/2}$	m 8.26 u 9.00	$\varepsilon(\sigma_g 5d) = 2.68$ eV[a,e]
	$^2\Pi_{u\ 1/2}$	u' 9.01	$\varepsilon(\sigma_g 5d) = 2.74$ eV[a,e]
	$^2\Sigma_u^-$	β 8.35 β' 8.36	$\varepsilon(\sigma_g 5d) = 2.4$ eV[c,d]
	$^2\Sigma_u^+$	η 8.85 η' 8.87	$\varepsilon(\sigma_g 5d) = 2.74$ eV[c,e]
$\pi_g 5d_{\pm 1}$	$^2\Pi_{u\ 3/2}$	p 8.38	$\varepsilon(\pi_g 5d) = 2.56$ eV[a,f]
	$^2\Pi_{u\ 1/2}$	w 9.10	$\varepsilon(\pi_g 5d) = 2.65$ eV[a,f]
	$^4\Sigma_u^-$	ζ 8.65 ζ' 8.67	$\varepsilon(\pi_g 5d) = 2.1$ eV[c,d]
	$^2\Delta_u$	ϑ 8.95	IP ($^2\Delta_u$) = 11.05 eV[d]

a) Calculated from IP values of 10.94 eV ($^2\Pi_{u\ 3/2}$) and 11.75 eV ($^2\Pi_{u\ 1/2}$). These are from photo-electron measurements [3,4] which were fitted at the first IP of Venkateswarlu [4].

b) calculated from $\varepsilon(\sigma_g 6s) = 3.05$ eV

c) calculated from IPs given in the table

d) reasonable value

e) two reasons why assignment must be wrong: it would mean an unreasonably small $(6s)\sigma_g 6s - (6p)\sigma_g 5d$ energy difference of 0.3 eV; the ε-values correspond to a minimum in the XUV-spectrum.

f) means that π_g lies 0.5 eV below π_u; this seems to be impossible.

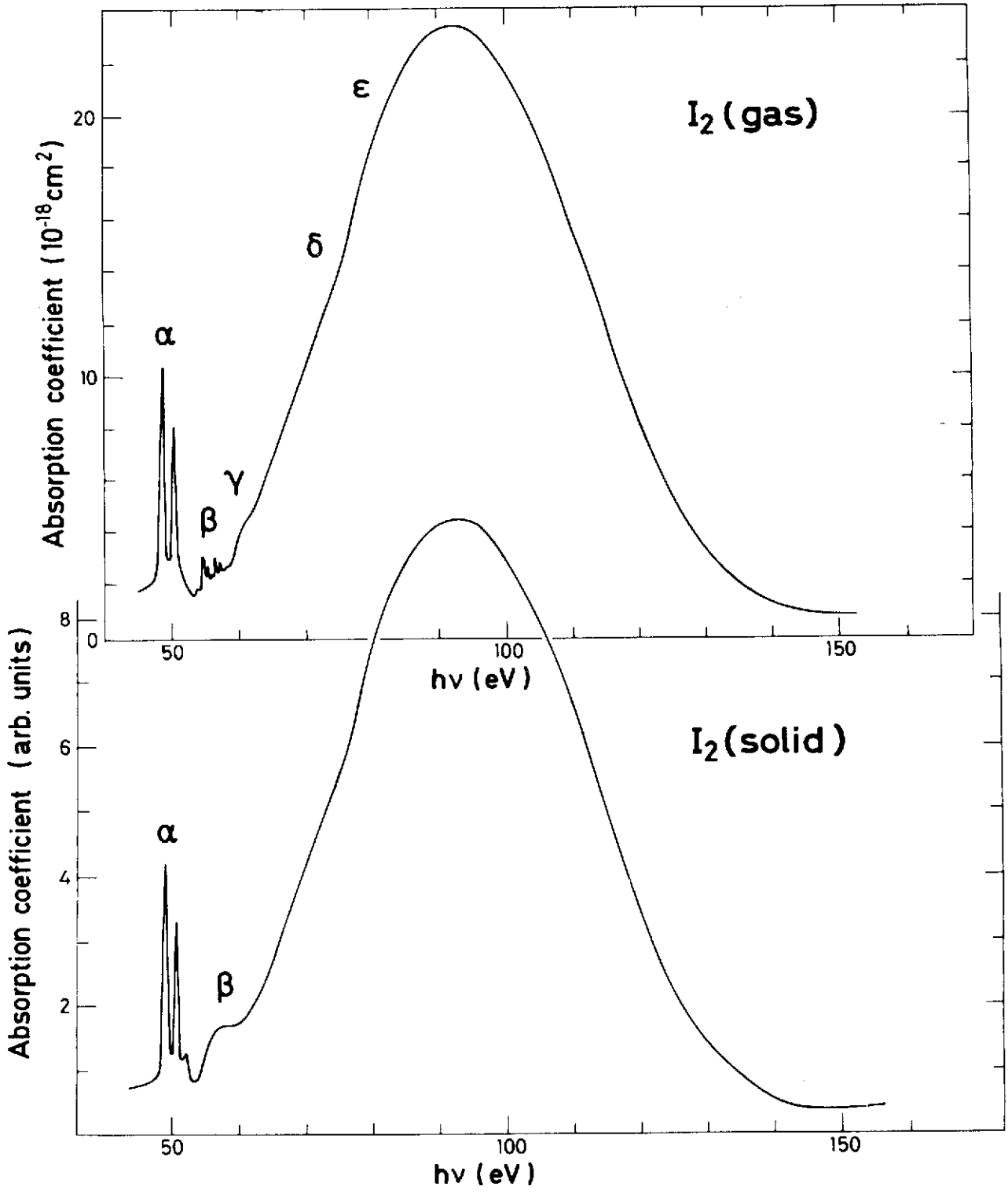
I2 (gas)
Absorption coefficient (10-18cm2)
20
10
0
α
β
γ
δ
ε
50
100
150
hν (eV)
I2(solid)
Absorption coefficient (arb. units)
8
6
4
2
α
β
50
100
150
hν (eV)

Fig.1

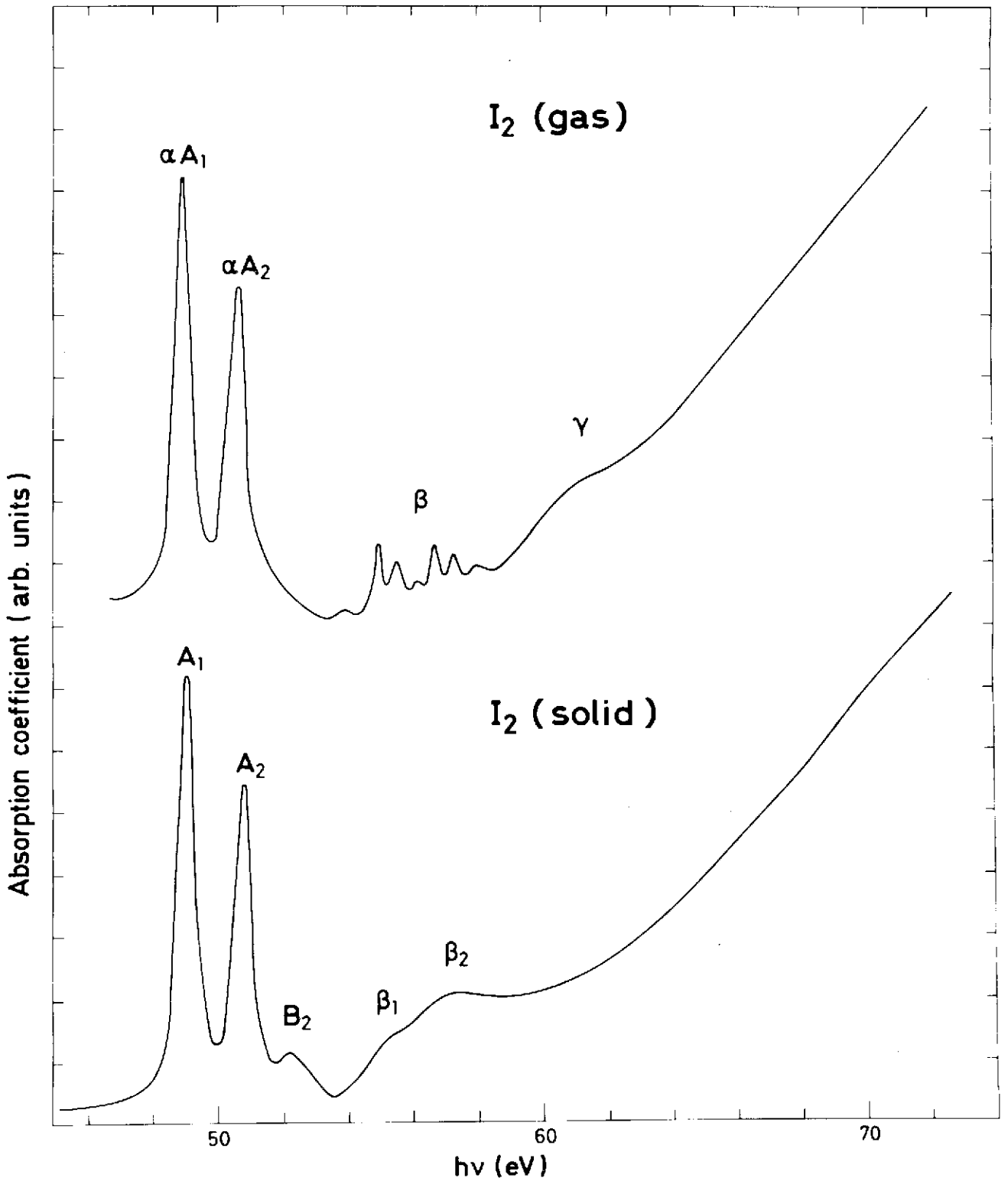
I2 (gas)
αA1
αA2
β
γ
I2 (solid)
A1
A2
B2
β1
β2
Absorption coefficient (arb. units)
50
60
70
hν (eV)

Fig.2

I2 (solid)
A1
A2
B1
B2
Absorption coefficient (arb. units)
49
50
51
52
hν (eV)

Fig.3

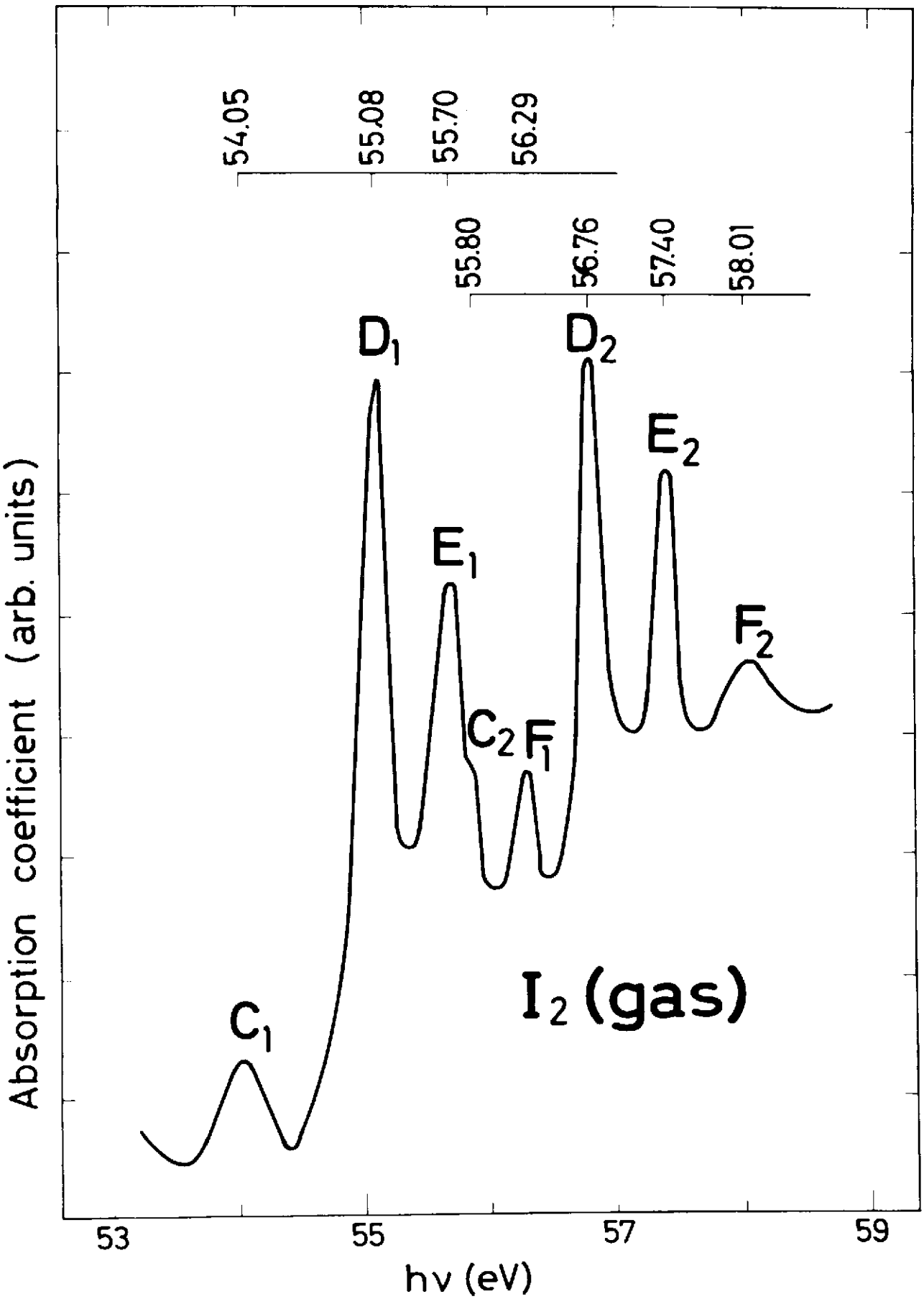
54.05
55.08
55.70
56.29
55.80
56.76
57.40
58.01
D1
D2
E2
E1
F2
C2
F1
C1
I2 (gas)
Absorption coefficient (arb. units)
53
55
57
59
hν (eV)

Fig.4

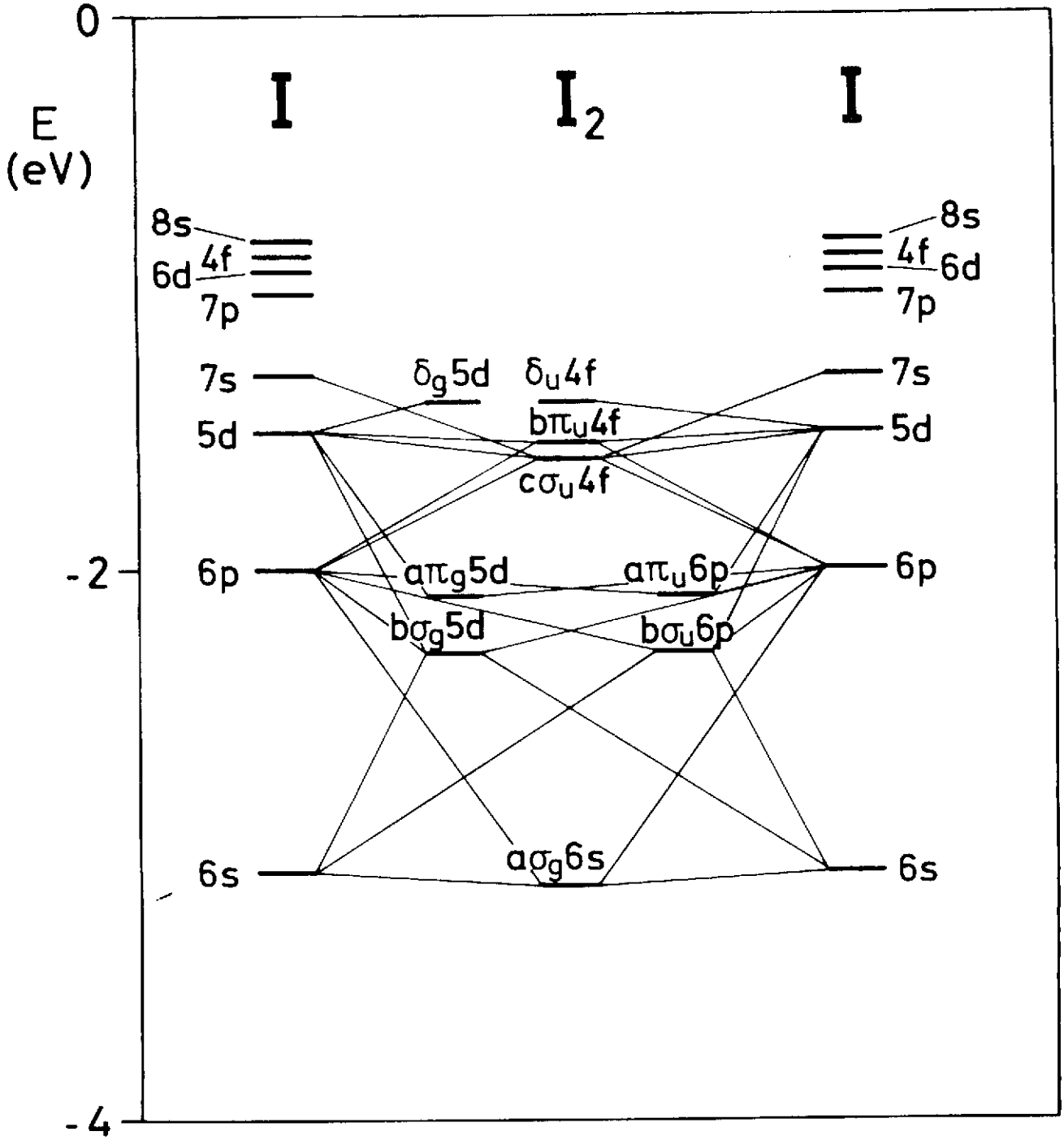
0
E
(eV)
-2
-4
I
I2
I
8s
4f
6d
7p
7s
5d
6p
6s
δg5d
δu4f
bπu4f
cσu4f
aπg5d
aπu6p
bσg5d
bσu6p
aσg6s

Fig. 5